Rearrangements in MLn complexes of diazenes and the ligand-substitution reaction

3 AUTHORS, INCLUDING:

Carlo Mealli
Italian National Research Council

245 PUBLICATIONS **5,142** CITATIONS

Contribution from the Department of Chemistry, University of Houston, Houston, Texas 77004,
and Istituto per lo Studio della Stereochemica ed Energetica dei Composti di Coordinazione, ISSECC-CNR, 50132 Firenze, Italy

Rearrangements in ML$_n$ Complexes of Diazenes and the Ligand-Substitution Reaction

Sung-Kwon Kang,[†] Thomas A. Albright,*[†] and Carlo Mealli[‡]

The rearrangement of a Cr(CO)$_5$ unit from one coordination site to another has been studied for *cis*- and *trans*-H$_2$N$_2$, pyridazine, naphthyridine, and phenanthroline complexes by means of extended Hückel calculations. The results for the 1,2-shift process in (*cis*-H$_2$N$_2$)Cr(CO)$_5$ were checked at the ab initio level and found to be in qualitative agreement with the extended Hückel calculations. In both isomers of H$_2$N$_2$ the favored reaction pathway is via a π-bonded species rather than a 20-electron complex (for the cis isomer) where the lone pairs on both nitrogens simultaneously interact with Cr(CO)$_5$. For pyridazine– and naphthyridine–Cr(CO)$_5$ the transition states are categorized by very long Cr–N distances; in other words, they contain substantial dissociative character. This study is extended to 16-electron square-planar analogues, namely pyridazine–, naphthyridine–, and phenanthroline–PtCl$_3^-$. The transition states in these cases are much more associative. Finally, a general analysis of ligand substitution at 18-electron complexes vs. nucleophilic substitution reactions in saturated, 8-electron compounds is developed. This analysis shows that ligand-substitution reactions at 18-electron ML$_n$ complexes, where L is a strong σ donor, are unlikely to proceed via an S$_N$2 transition state. This is entirely consistent with the numerical results for the diazene–Cr(CO)$_5$ complexes. In general a strong antibonding interaction between a filled metal d orbital and incoming ligand lone pair is turned on. In contrast, for organic/main group compound nucleophilic substitution reactions an S$_N$2 pathway is viable. The nucleophile lone-pair orbital evolves into a nonbonding orbital.

Introduction

The ligand-substitution reaction is probably the most important fundamental step in organometallic reaction mechanisms. The vast majority of proposed mechanisms require at least one ligand-substitution step, if not several steps. Recent comprehensive reviews[1] on the experimental details of organometallic ligand-substitution reactions indicate that while most information on 18-electron ML$_6$, ML$_5$, and ML$_4$ complexes is consistent with a dissociative mechanism proceeding via a 16-electron intermediate, there still is considerable ambiguity.[1,2] Little theoretical work has been brought to bear on this issue;[3] all of it has been confined to the computation of M–L bond dissociation energies and structural studies of 16-electron intermediates.

We have had a long-standing interest in haptotropic rearrangements,[4] wherein a ML$_n$ unit bonded to the π system of a polyene migrates from one coordination site to another. An obviously related reaction sequence, which has a direct bearing on the ligand-substitution reaction, is the rearrangement of an ML$_n$ unit from one coordination site to the other in a diazene complex. A description of the reactions covered in this work can be given in a generalized way for ML$_n$ = Cr(CO)$_5$. At the ground state one nitrogen lone pair interacts with Cr(CO)$_5$ to form a Cr–N σ bond, 1. Shifting the Cr(CO)$_5$ group to the other nitrogen
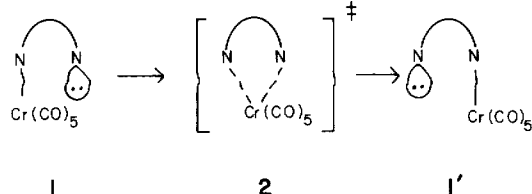
lone pair, 1′, requires passage through 2. Specific examples where this rearrangement has been experimentally investigated include Cr(CO)$_5$ complexes of azo compounds, 3,[5] phthalazine, 4,[6] and naphthyridine, 5.[6] Benzocinnoline[5a,6a,7] and imidazole[8] complexes
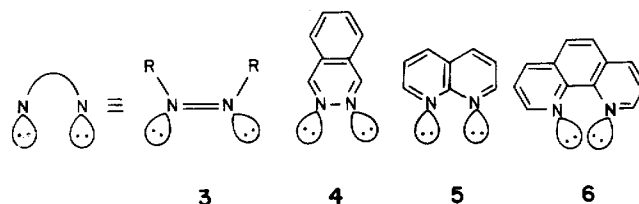
are other examples. No evidence exists for this rearrangement in Cr(CO)$_5$ complexes of 1,4-diazabutadienes,[9] and we are not aware of the synthesis of a phenanthroline complex, 6. However, ample experimental evidence does exist for square-planar, ML$_3$ complexes of both ligands.[10] This type of internal ligand sub-

(1) (a) Howell, J. A. S.; Burkinshaw, P. M. *Chem. Rev.* 1983, *83*, 557. (b) Dobson, G. R. *Acc. Chem. Res.* 1976, *9*, 300.
(2) See also: Basolo, F. *Inorg. Chim. Acta* 1985, *100*, 33; 1981, *50*, 65.
(3) For a review see: Dedieu, A. *Topics in Physical Organometallic Chemistry*; Gielen, M. F., Ed.; Freund: London, 1985; Vol 1, pp 1–141.
(4) (a) Hofmann, P.; Albright, T. A. *Angew. Chem.* 1980, *92*, 747. (b) Albright, T. A. *J. Organomet. Chem.* 1980, *198*, 159. (c) Albright, T. A.; Geiger, W. E.; Moraczewski, J.; Tulynathan, B. *J. Am. Chem. Soc.* 1981, *103*, 4787. (d) Mealli, C.; Midollini, S.; Moneti, S.; Sacconi, L.; Silvestre, J.; Albright, T. A. *Ibid.* 1982, *104*, 95. (e) Albright, T. A.; Hofmann, P.; Hoffmann, R.; Lillya, C. P.; Dobosch, P. A. *Ibid.* 1983, *105*, 3396. (f) Silverstre, J.; Albright, T. A. *Ibid.* 1985, *107*, 6829. (g) Karel, K. J.; Albright, T. A.; Brookhart, M. *Organometallics* 1982, *1*, 419. (h) Silvestre, J.; Albright, T. A. *Nouv. J. Chim.* 1985, *9*, 659.
(5) (a) Ackermann, M. N.; Willett, R. M.; Englert, M. H.; Barton, C. R.; Shewitz, D. B. *J. Organomet. Chem.* 1979, *175*, 205. (b) Ackermann, M. N.; Shewitz, D. B.; Barton, C. R. *Ibid.* 1977, *125*, C33. (c) Frazier, C. C., III; Kisch, H. *Inorg. Chem.* 1978, *17*, 2736. (d) Herberhold, M.; Leonhard, K. *Angew. Chem.* 1976, *88*, 227. (e) For isolobal benzene–Cr(CO)$_2$ complexes, see: Herberhold, M.; Leonhard, K.; Kreiter, C. G. *Chem. Ber.* 1974, *107*, 3222.
(6) (a) Dixon, K. R.; Eadie, D. J.; Stobart, S. R. *Inorg. Chem.* 1982, *21*, 4318. (b) Reed, T. E.; Hendricker, D. G. *J. Coord. Chem.* 1972, *2*, 83.
(7) Kooti, M.; Nixon, J. F. *J. Organomet. Chem.* 1976, *105*, 217.
(8) (a) Hog, M. F.; Johnson, C. R.; Paden, S.; Shepherd, R. E. *Inorg. Chem.* 1983, *22*, 2693. (b) Purcell, W. L. *Ibid.* 1983, *22*, 1205. (c) Ellis, W. R., Jr.; Purcell, W. L. *Ibid.* 1982, *21*, 834. (d) Balahura, R. J.; Purcell, W. L.; Victoriano, M. E.; Lieberman, M. L.; Loyola, V. M.; Fleming, W.; Fronabarger, J. W. *Ibid.* 1983, *22*, 3602.
(9) (a) Schadt, M. J.; Lees, A. J. *Inorg. Chem.* 1986, *25*, 672. (b) Schadt, M. J.; Gresalfi, N. J.; Lees, A. J. *Ibid.* 1985, *24*, 2942.

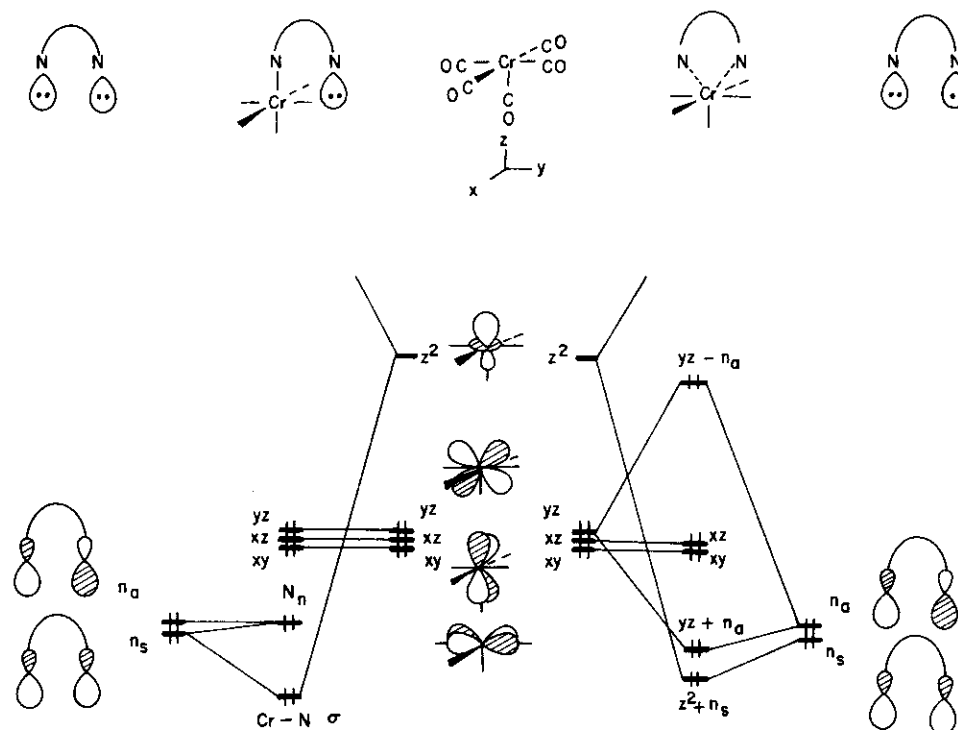[†] University of Houston.
[‡] ISSECC-CNR.

Figure 1. Interaction diagrams for the ground (1) and transition state (2) in a generalized diazene–Cr(CO)$_5$ complex.

stitution reaction is by no means confined to diazenes. The elegant work of Abel, Orrell, and co-workers[11] has established that [1,2]- and [1,3]-shifts are possible for di- and trithio complexes of Cr(CO)$_5$, etc.

Diazene–ML$_n$ rearrangements are interesting models of the ligand-substitution reaction. First of all, in a normal L′ + ML$_n$ → ML′L$_{n-1}$ + L reaction there is an intrinsic entropy bias for a dissociative (S$_N$1) mechanism over an associative (S$_N$2) process (ΔS‡ is expected to be much more positive for the former). Tying the incoming ligand to the outgoing one in the 1–1′ reaction largely removes this entropy bias. Furthermore, in the 3–6 series and for internal ligands substitution reactions in general, the lone-pair orientations are fixed primarily by the geometry of the bidentate ligand itself. This restriction of the reaction path for the L′ + ML$_n$ reaction is, of course, removed. To put this another way, the geometrically enforced rigidity of the lone-pair orientations in 3–6 can be used as experimental and theoretical probes of differing reaction trajectories for the ligand-substitution reaction. Before we discuss the specific details associated with the rearrangement in Cr(CO)$_5$ complexes of 3–6, it is useful to pursue the 1–1′ reaction further and develop a generalized theoretical model for this internal ligand-substitution reaction, which will then

be used to view our computational results. Our extended Hückel and ab initio results indicate that the transition states for the diazene–Cr(CO)$_5$ series are very dissociative (near the S$_N$1 limit). As previously mentioned, this feature is also prominent for most ligand substitution reactions of 18-electron complexes. Yet, in organic and main group chemistry the S$_N$2 mechanism is quite common. In the last section of the paper we shall address this issue from two perspectives: one focuses on the differences at the transition state for an associative S$_N$2 mechanism and the other concentrates on differences at the early stages of reaction.

Generalized Model of Diazene Rearrangements

Figure 1 shows the interaction diagram for an idealized diazene ligand and a Cr(CO)$_5$ fragment in the ground state (1) and the transition state (2). At the far left and right of Figure are symmetry-adapted linear combinations of the lone-pair hybrids on each nitrogen atom, n$_s$ and n$_a$. For the time being we shall consider that the interaction between the hybrids is small so that the n$_s$–n$_a$ splitting is small. In the center of Figure 1 are the four metal-centered orbitals of a Cr(CO)$_5$ fragment.[12] At low energy are three filled t$_{2g}$-like orbitals, xy, xz, and yz (the coordinate system is given at the top of Figure 1). At higher energy is an empty level primarily of z^2 character. It is hybridized with metal s and z so that it extends away from the CO ligands, toward the empty coordination site. At the ground-state geometry, 1, (left side of Figure 1) xy, xz, and yz remain nonbonding. They form the t$_{2g}$ set of this octahedral complex. The n$_s$ and n$_a$ combinations overlap with z^2 to form a typical three-orbital pattern. At low energy n$_s$ and n$_a$ mix with z^2 in a bonding fashion to produce a Cr–N σ bond, 7. At higher energy n$_a$ interacts with z^2 in a bonding fashion; however, n$_s$ enters in an antibonding way with respect to z^2. The resultant orbital is primarily localized on the uncoordinated nitrogen atom, 8. At much higher energy, not shown in Figure 1, n$_s$ and n$_a$ both interact with z^2 in an antibonding fashion to produce a Cr–N σ* orbital. What we have done simply is to localize the linear combination of nitrogen lone-pair hybrids on each nitrogen and form from them a Cr–N σ bond and a nonbonding nitrogen lone pair. The situation is different for the transition state of this rearrangement, 2 (on the right side of Figure 1). The xz and xy orbitals remain nonbonding. The n$_s$ lone pair combination overlaps with z^2 to produce a bonding (labeled z^2 + n$_s$) and a high-lying, empty antibonding molecular orbital (not shown in Figure 1). A critical feature of this qualitative analysis is that n$_a$ overlaps with

(10) (a) Brandon, J. B.; Collins, M.; Dixon, K. R. *Can. J. Chem.* **1978**, *56*, 950. (b) Dixon, K. R. *Inorg. Chem.* **1977**, *16*, 2618. (c) Bushnell, G. W.; Dixon, K. R.; Khan, M. A. *Can. J. Chem.* **1974**, *52*, 1367. (d) Schmidbaur, H.; Dash, K. C. *J. Am. Chem. Soc.* **1973**, *95*, 4855. (e) van der Poel, H.; van Koten, G.; Vrieze, K. *Inorg. Chem.* **1980**, *19*, 1145. (f) van Koten, G.; Vrieze, K. *Recl. J. R. Neth. Chem. Soc.* **1981**, *100*, 129 and references therein.

(11) (a) Abel, E. W.; Bhargava, S. K.; Orrell, K. G. *Prog. Inorg. Chem.* **1984**, *32*, 1. (b) Abel, E. W.; Bhargava, S. K.; MacKenzie, T. E.; Mittal, P. K.; Orrell, K. G.; Sik, V. *J. Chem. Soc., Chem. Commun.* **1982**, 983. (c) Abel, E. W.; Bhargava, S. K.; Mittal, P. K.; Orrell, K. G.; Sik, V. *Ibid.* **1982**, 535. (d) Abel, E. W.; Booth, M.; Orrell, K. G.; Pring, G. M.; Cameron, T. S. *Ibid.* **1981**, 29. (e) Abel, E. W.; Chowdhury, M. A. Z.; Orrell, K. G.; Sik, V. *J. Organomet. Chem.* **1984**, *262*, 293. (f) Abel, E. W.; King, G. D.; Orrell, K. G.; Pring, G. M.; Sik, V.; Cameron, T. S. *Polyhedron* **1983**, *2*, 1117. (g) Abel, E. W.; King, G. D.; Orrell, K. G.; Sik, V. *Ibid.* **1983**, *2*, 1363. (h) Abel, E. W.; Booth, M.; Orrell, K. G.; Pring, G. M. *J. Chem. Soc., Dalton Trans.* **1981**, 1944. (i) Abel, E. W.; Bhargava, S. K.; Mittal, P. K.; Orrell, K. G.; Sik, V. *Ibid.* **1985**, 1561. (j) Abel, E. W.; Mittal, P. K.; Orrell, K. G.; Sik, V. *Ibid.* **1985**, 1569. (k) Abel, E. W.; Higgins, K. M.; Orrell, K. G.; Sik, V.; Curzon, E. H.; Howarth, O. W. *Ibid.* **1985**, 2195. (l) Pogorzelec, P. J.; Reid, D. H. *J. Chem. Soc., Chem. Commun.* **1983**, 289.
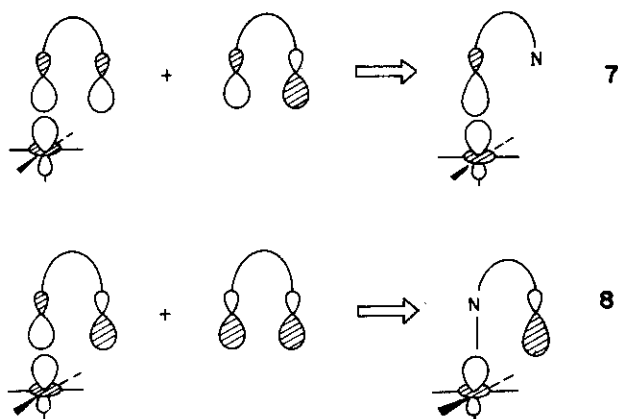
yz to produce *filled* bonding ($yz + n_a$) and antibonding ($yz - n_a$) molecular orbitals. Elementary perturbation theory considerations[12a] tell us that the antibonding combination is destabilized more than the bonding combination is stabilized; therefore, the net interaction between *yz* and n_a is repulsive. This is shown more clearly from an idealized Walsh diagram for the rearrangement given in Figure 2. The N_n orbital smoothly transforms into *yz* + n_a and is stabilized. On the other hand, the *yz* orbital rises to a very high energy, ultimately yielding $yz - n_a$; the destabilization of this molecular orbital along the reaction path offsets the stabilization in $yz + n_a$. This is the predominant factor that sets an energy barrier on going from **1** to **2**. The magnitude of this net destabilization is proportional to the overlap between *yz* and n_a.[12a] An obvious way to decrease the overlap would be to allow the Cr–N distance to increase going from **1** to **2**. Then molecular *yz* and N_n would not respectively rise and fall much in energy. The problem is that at long Cr–N distances in **2** the overlap between n_s and z^2 will also become small. Hence, the Cr–N σ bond will rise to a high energy (in the limiting case to approximately the same energy as N_n). Notice that in fact the idealized Walsh diagram shows a slight destabilization of this molecular orbital. In part this reflects the assumption that the Cr–N distances in **2** will be longer than the Cr–N bonded distance in **1**. There is another factor that is also important. In this generalized case the lone pairs on the nitrogens are oriented in a parallel fashion. They lie close to the nodal plane of z^2 at **2**, see $z^2 + n_s$ in Figure 2. This also serves to decrease the overlap between z^2 and n_s and consequently to destabilize this molecular orbital.

There are two additional factors that should be discussed in the context of this generalized model. First of all, there is no reason to restrict the orientation of the lone pairs on the nitrogen. While the example we have covered represents a very simplified view of naphthyridine, **5**, in that the lone pairs on the nitrogens are parallel, clearly **9** is a better representation for **3**, **4**, or other

9   **10**

diazenes where the lone pairs are directed away from each other and **10** is a better model for **6** or diazenes where the lone pairs are pointed toward each other. It is easy to see that the overlap between the n_s combination in **10** and z^2 is intrinsically larger than the n_s/z^2 overlap in **9** (for a fixed set of Cr–N distances). Therefore, one would expect that a diazene like **10** should show more associative character for the rearrangement reaction (the Cr–N distances should be shorter at the transition state) than the analogous reaction for a diazene like **9**. The variation of overlap between n_a and *yz* with respect to the lone-pair orientation is more difficult to predict a priori. It depends not only on the Cr–N
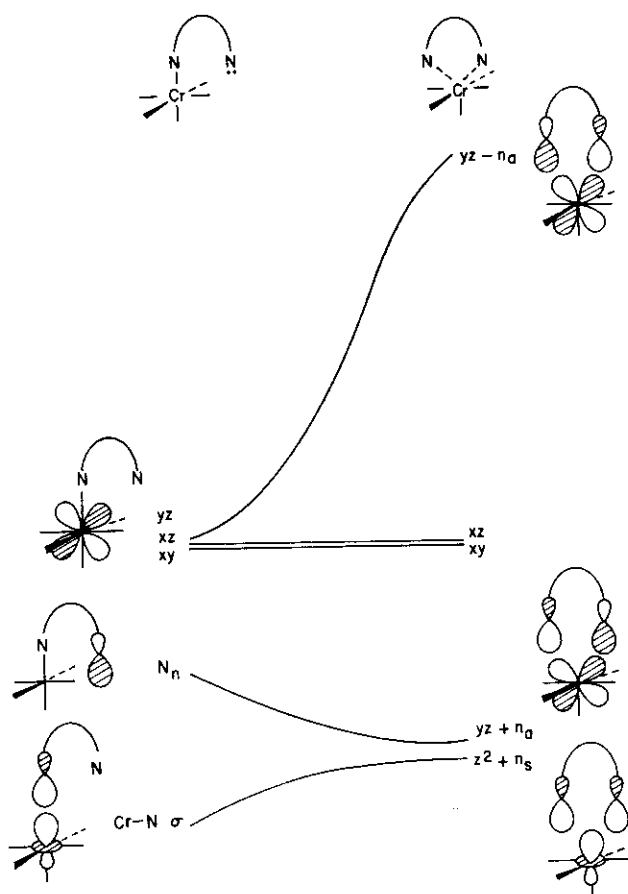

Figure 2. Idealized Walsh diagram for the **1 → 2** reaction.

distances at the transition state but also on the N⋯N distance. For realistic cases, the n_a/*yz* overlap in **9** is smaller than that in **10**. Recall from the previous discussion that *minimizing* the n_a/*yz* overlap will stabilize the transition state. Thus, there are two competing trends for how the lone-pair orientation affects the relative energy and associated geometry of the transition state. Calculations on $(NH_3)_2Cr(CO)_5$ as a model for the **1 → 2** reaction and vide infra indicate minimizing n_a/*yz* overlap is slightly more important than maximizing n_s/z^2 overlap. The second factor is the degree to which the lone pairs interact with each other. Our previous discussion tacitly assumed that there was none. There are two mechanisms by which the lone pairs interact. The most simple is a direct, through-space interaction. The magnitude of this effect is sensitive to the N⋯N distance and lone-pair orientation. As the two nitrogen atoms are brought closer together, there is a larger interaction; consequently, the n_s combination is stabilized and n_a is pushed to higher energy. An identical situation occurs as the lone pairs are swiveled toward each other. Through-bond conjugation[12a,13] can modify this result. Here the intervening σ system overlaps with n_s and/or n_a. The most interesting situation arises when the highest occupied σ orbital has the correct symmetry and destabilizes n_s. In fact the n_s combination can be at a higher energy than n_a.[13] Our concern with how through-space and through-bond conjugation modify the energy of n_s and n_a is easily understood by referring back to the generalized interaction diagram for the transition state (right side of Figure 1). Either type of conjugation that destabilizes n_s makes it a better donor orbital to z^2; i.e. the z^2/n_s energy difference decreases so the interaction between the two is larger and the transition state becomes more stable.

The salient features of this generalized analysis can be summarized as follows:

(12) (a) Albright, T. A.; Burdett, J. K.; Whangbo, M.-H. *Orbital Interactions in Chemistry*; Wiley: New York, 1985. (b) Elian, M.; Hoffmann, R. *Inorg. Chem.* **1975**, *14*, 1058. (c) Albright, T. A.; Hoffmann, R.; Thibeault, J. C.; Thorn, D. L. *J. Am. Chem. Soc.* **1979**, *101*, 3801.

(13) (a) Hoffmann, R. *Acc. Chem. Res.* **1971**, *4*, 1. (b) Gleiter, R. *Angew. Chem.* **1974**, *86*, 770. (c) Martin, H.-D.; Mayer, B. *Ibid.* **1983**, *95*, 281. (d) Lee, I. *Tetrahedron* **1983**, *39*, 2409.

1. The largest source of the energy barrier for this rearrangement is associated with repulsion between the nitrogen lone pairs and one filled member of the t$_{2g}$ set at the metal.

2. Barring other factors, as the lone pairs are forced to point away from each other, the transition state should become more associative in nature.

3. A consideration of through-space interaction between the two lone pairs leads to the same result.

4. If through-bond conjugation operates to destabilize n$_s$, then the transition state will be more associative.

We now proceed to specific systems.

Azo Complexes

A variety of *cis*- and *trans*-azo complexes of Cr(CO)$_5$, **11** and **12**, respectively, are known.[5,14] Ackermann and co-workers have
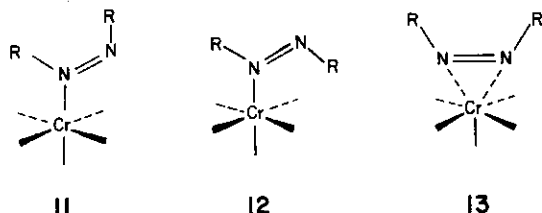
measured the barrier of a [1,2]-shift when R = isopropyl at 15.0 kcal/mol[5a] for the cis complex. Good evidence exists for a non-dissociative route, and a transition state akin to **13** was proposed.[5a] We have carried out extended Hückel calculations on the parent azo complex (R = H). Computational and geometric details are given in the Appendix. The optimized Cr–N distance in **11** was found to be 1.91 Å. This is probably somewhat too short. While no structural data exists for an azo–Cr(CO)$_5$ complex, the Cr–N bond lengths in pyridine–Cr(CO)$_5$ and bis(pyridine)–Cr(CO)$_4$ are 2.16 Å.[15] The molecular orbitals for **11** have been given in a qualitative fashion elsewhere[5a,5c] as well as for the isoelectronic Cr(CO)$_5$ complexes of H$_2$P$_2$[16] and HP=CH$_2$.[17] The basic features are shown in fact on the left side of Figure 1. Although the two lone pairs in the ligand are pointed away from each other, since they are on adjacent nitrogen atoms, there is a strong through-space interaction (no through-bond conjugation can take place); thus, n$_s$ lies well below n$_a$. Our calculations put n$_s$ at −14.5 and n$_a$ at −12.6 eV. Additionally there is some, albeit small, back-donation from *xz* into the low-lying π^* orbital of H$_2$N$_2$. At the transition state the Cr–N distances optimized to be 2.85 Å. The energy of **13** was 39 kcal/mol higher than the ground state. There is certainly a great discrepancy between the experimental and theoretical numbers. Part of this is due to the method; however, part is due to the reaction path we have chosen. The binding energy between H$_2$N$_2$ and Cr(CO)$_5$ at the ground state will greatly influence the actual magnitude of the barrier. Provided there is significant ligand–metal bond breaking at the transition state, which is the case for all of these rearrangements, if the binding energy is large then the corresponding activation energy will also be large and vice versa. We do *not* expect the extended Hückel method to give us reliable binding energies. In fact it is computed to be 45 kcal/mol for **11**. This is clearly much too large; a more reasonable value would be ≈25 kcal/mol.[18] Therefore, a portion of the unreasonably large activation energy is due to the overestimation of the H$_2$N$_2$/Cr(CO)$_5$ binding energy for the ground state by the extended Hückel method. What is more significant in a theoretical (and experimental) context is to de-

termine how much bonding is lost on going from the ground to transition state. The elongation of the Cr–N distance from 1.91 to 2.85 Å certainly indicates substantial bond breakage. On an energetic basis 87% of the bond energy at the ground state is required to reach **13**. We have checked this by carrying out computations of (H$_2$N$_2$)Cr(CO)$_5$ at the ab initio level. Computational and basis set details are given in the Appendix. The optimized Cr–N distance at the ground state was 2.16 Å, in good agreement with Cr–N distances in pyridine complexes.[15] At the transition state, **13**, the optimal Cr–N distances were 2.85 Å, identical with the extended Hückel results. The corresponding activation energy was 17.2 kcal/mol. The binding energy between H$_2$N$_2$ and Cr(CO)$_5$ at the ground state was approximately 20 kcal/mol. This value at the Hartree–Fock level is underestimated for well-known reasons.[3,19] What is interesting is that it requires 86% of the binding energy to reach the transition state; a percentage very close to that predicted at the extended Hückel level. The results at both levels indicate very clearly that the repulsion between n$_a$ and *yz* is the culprit. The ab initio optimized value for the N–N distance at the transition state was 1.24 Å, slightly enlarged from the 1.22 Å for *cis*-H$_2$N$_2$ itself.[20] The H–N–N angles of 116° are identical with that for free *cis*-H$_2$N$_2$.[20] The same is true at the extended Hückel level. The H–N–N angles of 120° at the transition state are identical with those optimized for *cis*-H$_2$N$_2$. In other words, there is no tendency for the lone pairs to swivel toward each other to minimize the z^2/n_s overlap.

We have also checked via extended Hückel calculations on possible distortions within the Cr(CO)$_5$ framework for the transition state, **13**. Rotation of the H$_2$N$_2$ unit to **14** requires a tiny,
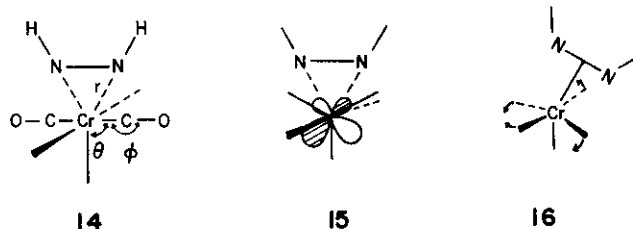
1.4-kcal/mol barrier. Bending the two CO units that are eclipsed by H$_2$N$_2$ *toward* H$_2$N$_2$ rehybridizes *yz* to that shown in **15**.[12a,21] Furthermore, bending the Cr–C–O angle can cause a net transfer of electron density to the CO π^* system, an effect that Basolo has proposed for ligand-substitution reactions with associative character.[2] Unfortunately, we find that the optimal values of *r*, θ, and ϕ (defined in **14**) were 2.86 Å, 93°, and 177°, respectively. The energy gain by these optimizations was only 0.4 kcal/mol. We also explored distortions toward a pentagonal bipyramid, **16**. None were found to be stabilizing.

A completely different reaction path involves passage through a π complex, **17**. Ample precedent exists for this coordination
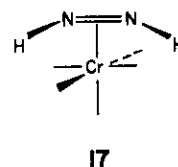
mode in the literature for other transition-metal complexes.[22]

(14) For reviews see: (a) Albini, A.; Kisch, H. *Top. Curr. Chem.* **1976**, *65*, 105. (b) Carty, A. J. *Organomet. Chem. Rev., Sect. A* **1972**, *7*, 191. (c) Kilmer, M. *Organomet. Chem.* **1972**, *10*, 115.

(15) Reis, W.; Bernal, I.; Quast, M.; Albright, T. A. *Inorg. Chim. Acta* **1984**, *83*, 5.

(16) Schugart, K. A.; Fenske, R. F. *J. Am. Chem. Soc.* **1985**, *107*, 3384.

(17) Nguyen, M. T.; McGinn, M. A.; Hegarty, A. F. *Organometallics* **1986**, *5*, 1223.

(18) This is the binding energy of pyridine to Cr(CO)$_5$, see: Dennenberg, R. J.; Darensbourg, D. J. *Inorg. Chem.* **1972**, *11*, 72. The Cr–N bond energy in tetracarbonyl(1-(diphenylphosphino)-3-(dimethylamino)-propane)chromium was measured to be 27.5 ± 1.2 kcal/mol: Dobson, G., private communication.

(19) See, for example: Sauer, J.; Haberlandt, H.; Pacchioni, G. *J. Phys. Chem.* **1986**, *90*, 3051 and references therein.

(20) See ref 98 in: Howell, J. M.; Kirschenbaum, L. J. *J. Am. Chem. Soc.* **1976**, *98*, 877.

(21) Kubacek, P.; Hoffmann, R. *J. Am. Chem. Soc.* **1981**, *103*, 4320.

(22) (a) Dickson, R. S.; Ibers, J. A.; Otsuka, S.; Tatsuno, Y. *J. Am. Chem. Soc.* **1971**, *93*, 4636; **1972**, *94*, 2988. Nakamura, A.; Yoshida, T.; Cowie, M.; Otsuka, S.; Ibers, J. A. *Ibid.* **1977**, *99*, 2108. Ittel, S. D.; Ibers, J. A. *J. Organomet. Chem.* **1973**, *57*, 389; *Inorg. Chem.* **1975**, *14*, 1183. (b) Jacob, M.; Weiss, E. *J. Organomet. Chem.* **1978**, *153*, 31. (c) Elmes, P. S.; Leverett, P.; West, B. O. *J. Chem. Soc. D* **1971**, 747. (d) Fochi, G.; Floriani, C.; Bart, J. C. J.; Giunchi, G. *J. Chem. Soc. Dalton Trans.* **1983**, 1515. Bart, J. C. J.; Bassi, I. W.; Ceruti, G. F.; Calcaterra, M. *Gazz. Chim. Ital.* **1980**, *110*, 423. (e) Deppisch, B.; Schäfer, H. *Acta Crystallogr., Sect. B: Struct. Crystallogr. Cryst. Chem.* **1982**, *B38*, 748.
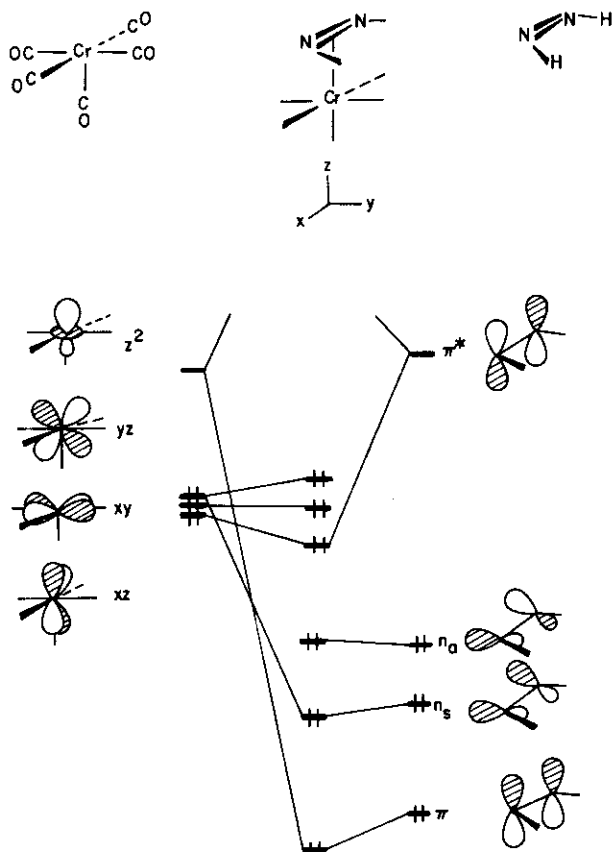
**Figure 3.** Interaction diagram for $(H_2N_2)Cr(CO)_5$ at the π-coordinated geometry.

Figure 3 shows an interaction diagram for the molecule at a slightly different perspective. Bonding with the z^2 acceptor orbital on $Cr(CO)_5$ now takes place via the π level of H_2N_2. It is important to realize that the interaction here is not nearly as strong as that between n_s and n_a at the ground-state geometry, primarily for energy gap reasons. The n_s and n_a orbitals lie at a higher energy than π does; consequently, they are closer to z^2. There is some destabilization between yz and n_s (and an even smaller one between xy and n_a), but this is not nearly as large as the yz/n_a destabilization in **13** for overlap reasons. The significant difference between transition states **13** and **17**[23] is the stabilization of xz by the low-lying π^* orbital of H_2N_2 in the latter. The much larger occupation of π^* at **17** compared to the ground state is reflected at the ab initio level by an elongation of the optimal N–N distance. We compute it to be 1.27 Å in **17**, whereas it is 1.23 Å in the ground state. **17** is, therefore, much like an olefin–$Cr(CO)_5$ complex. The optimal orientation of the H_2N_2 unit, where the N–N axis eclipses two Cr–CO bonds, is derived from the same basis as that found for olefin–ML_5 complexes.[12c] Likewise, the hydrogens do not lie in a plane parallel to the $Cr(CO)_4$ unit. Instead they bend away from the metal: 27° at the extended Hückel level and 19° at the ab initio level. This key feature creates a transition state with much more associative character and a lower energy than that given by **13**. The ab initio Cr–N distance was 2.37 Å for **17** at an energy 13.5 kcal/mol higher than the ground state (67% of the H_2N_2–$Cr(CO)_5$ bond energy is lost). The extended Hückel calculations yield an optimal Cr–N distance of

2.19 Å with a 25 kcal/mol energy difference (56% of the bond dissociation energy).[24]

Our conclusion is that the reaction path for the [1,2]-shift in azo–$Cr(CO)_5$ complexes occurs via the π complex, **17**, rather than the 20-electron species, **13**. If this is true, then an analogous rearrangement should occur for $(trans\text{-}H_2N_2)Cr(CO)_5$, **12**. Extended Hückel calculations put the activation energy required to reach the π complex at 27 kcal/mol (60% of the bond dissociation energy). This barrier is slightly larger than that for the cis complex. The yz level is now destabilized by the n_a combination (in C_2 symmetry) at the transition state, and this in turn is slightly larger than the yz/n_s repulsion for the cis complex. However, we think that the rearrangement should be experimentally viable. Fluxionality has not been observed for $trans$-azo–$M(CO)_5$ complexes via NMR line broadening.[5] We encourage a reinvestigation using NMR methods not based on coalescence. Substituents on the azo group (for both cis and trans isomers) that lower the energy of π^*, e.g. acyl or fluoro, should lower the activation energy for this path.

Heterocyclic Diazene Complexes

In this portion of the paper all computations have been carried out at the extended Hückel level. As a model for the phthalazine ligand, **4**, we have chosen pyridazine, **18**. There is again very
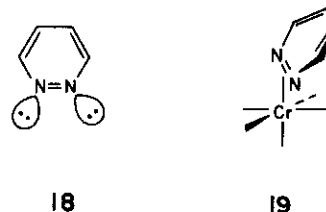
strong through-space interaction; n_a is above n_s by approximately 2 eV by experiment[25] and our calculations. The lone pairs are oriented in essentially the same direction as in the cis-azo ligands. Therefore, the behavior of pyridazine–$Cr(CO)_5$ should correspond quite closely to that found for $(cis\text{-}H_2N_2)Cr(CO)_5$. The optimum Cr–N bond length at the ground state was found to be 2.10 Å. At the transition state, **19**, this enlarges to 2.80 Å and it requires 85% of the bond dissociation energy (29 kcal/mol). The pyridazine ligand is tilted 50° from the plane parallel to the $Cr(CO)_4$ plane. In other words, the transition state structurally lies between **13** and **17** in $(cis\text{-}H_2N_2)Cr(CO)_5$. The reason behind this lies in the fact that the π^* orbital of pyridazine lies at a higher energy than that for cis-H_2N_2 and this leads to a smaller interaction with xz.[26] Our prediction is that the barrier for pyridazine–$Cr(CO)_5$ should be larger and proceed via more dissociative character than that for a cis-azo–$Cr(CO)_5$ complex. This appears to be true. The reported barrier for phthalazine–$Cr(CO)_5$ was 18.9 kcal/mol[6a,27] while that for **11**, R = i-Pr, was 15 kcal/mol.[5a]

In naphthyridine, **5**, the lone pairs are swiveled so that they are approximately parallel to each other. This should lead to a more dissociative transition state and a larger barrier. On the other hand, through-space overlap between the lone pairs is diminished since the nitrogens are no longer adjacent. Furthermore,

(23) Extended Hückel calculations on model transits from the ground state to **17**, which involve a concerted folding and sliding motion of the H_2N_2 ligand relative to the $Cr(CO)_5$ group, do not indicate that a barrier should exist between these two structures. However, we cannot discount the possibility that **17** is an intermediate separated by a small barrier for collapse back to the ground state. It has recently been demonstrated that interconversion occurs between η^1 isomers in the isolobal CpRe-$(CO)_2$ complex of $trans$-azobenzene by way of an η^2 intermediate; in fact, the crystal structure of the latter isomer has been determined, see: Einstein, F. W. B.; Sutton, D.; Tyers, K. G. *Inorg. Chem.* **1987**, *26*, 111.

(24) It is interesting to note that if one accepts 25 kcal/mol[18] as dissociation energy and $\approx$60% loss is required to attain the transition state **17**, then the corresponding barrier should be 15 kcal/mol. This is identical with the experimental barrier for **11**, R = i-Pr.[5a]

(25) Gleiter, R.; Heilbronner, E.; Hornung, V. *Angew. Chem.* **1970**, *82*, 878.

(26) The comparison here should be made for the energy of π^* at the transition-state geometry, i.e. for a N–N distance of $\approx$1.27 Å in H_2N_2. In the worst possible case, an N–N distance of 1.25 Å in H_2N_2 and 1.41 Å in pyridazine, the computed energies of π^* are −10.79 and −10.37 eV, respectively. Furthermore, the π^* level in pyridazine is substantially delocalized over the four arene carbons as well as the two nitrogens. In H_2N_2 π^* is, of course, localized on the two nitrogens. Therefore, there is an intrinsically smaller overlap between π^* and xz for the pyridazine complex.

(27) Using 25 kcal/mol as the phthalazine–$Cr(CO)_5$ bond energy and our calculated value of 85% for the bond energy lost upon reaching the transition state leads to an activation energy of 21 kcal/mol. This perhaps signals that our calculations are slightly overestimating the dissociative character in this rearrangement.

there is very strong through-bond coupling; n_s lies *above* n_a by ≈ 0.7 eV.[28] These factors should operate in opposite directions. At the ground state for naphthyridine–Cr(CO)$_5$, we compute the Cr–N bond distance to be 2.25 Å. At the transition state, **20**,
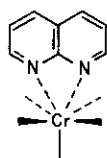
20

the optimal Cr–N distance was 3.15 Å and 77% of the bond dissociation energy was required to reach it (20 kcal/mol). A transit via the π system as well as paths toward a pentagonal bipyramid was found to be of higher energy. Our idea that through-bond conjugation will allow **20** to have more associative character is partially borne out. The most meaningful comparison can be made to **13** where 87% of the bond energy was lost at the transition state. The experimental barrier for naphthyridine–Cr(CO)$_5$ was found to be 14.0 kcal/mol,[6a,29] whereas that for phthalazine–Cr(CO)$_5$ is significantly larger (18.9 kcal/mol). On the other hand, the extremely long Cr–N distances in **20** argues that the interaction between the two units is tiny. We shall return to this point in the next section. We should also note that a recent paper by Alvarez, Bermejo, and Vinaixa[30] also examines rearrangements in ML$_5$ complexes of **4**, **5**, and other diazenes at the extended Hückel level. The reader is directed to this account in particular for an examination of electronegativity effects at the ligand.

In the phenanthroline ligand, **6**, the lone pairs are pointed toward each other. Through-space and through-bond interaction is strong; we compute that n_s lies just slightly above n_a. Optimization of the ground state for phenanthroline–Cr(CO)$_5$, **21**,
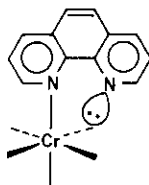
21

yields an interesting result. The optimal Cr–N distance was found to be quite long—2.50 Å. Furthermore, the optimal overlap of z^2 with n_s and n_a (see Figure 1) would require the two Cr–N–C angles to be approximately 120°. Instead, the Cr(CO)$_5$ unit is bent as shown in **21** so that one Cr–N–C angle is 100° and the other is 140°. There are obviously steric problems associated with the cis carbonyls and the phenanthroline ligand. There is also significant repulsion between the lone pair at the uncoordinated nitrogen and two members of the filled "t_{2g}" set at chromium (see
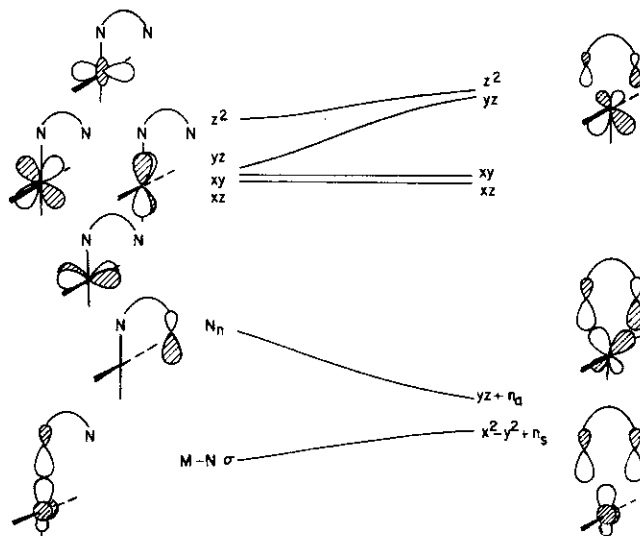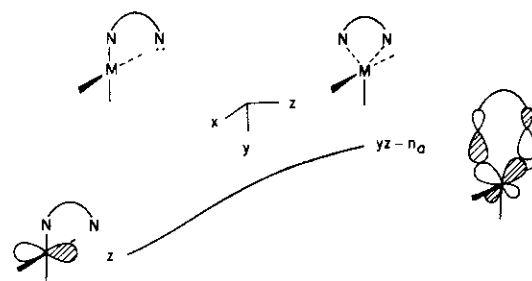

Figure 4. Idealized Walsh diagram for the rearrangement in a 16-electron diazene–ML$_3$ complex.

Figures 1 and 2). Both factors serve to elongate the Cr–N distance and rock the Cr(CO)$_5$ in a direction away from the uncoordinated lone pair. This leads to an extraordinarily small computed Cr–N bond energy of 10 kcal/mol. Given the crude nature of the extended Hückel method, this result by itself is perhaps not surprising. However, the careful reader will have noticed that all of the other diazene complexes had Cr–N bond dissociation energies that were calculated to be much too large at this computational level. It is reasonable that this is also the case for phenanthroline–Cr(CO)$_5$. Thus, we doubt that this complex is capable of existence for any meaningful period of time.[9] Fluxionality becomes a moot question. As mentioned in the Introduction a *monodentate* phenanthroline–ML$_5$ complex appears to be unknown. A large number of *bidentate* phenanthroline–ML$_4$ complexes do exist.[1,31]

It is tempting to speculate how the framework of a heterocyclic diazene can be modified to build in more associative character for the transition state in this rearrangement. The series of annelated bipyridines shown in **22** have been synthesized for n
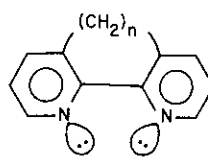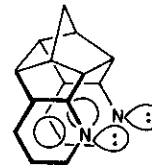
22   **23**

$= 0$–4.[32] The situation for $n = 2$ should be very similar to

(28) Jordan, A. D.; Ross, I. G.; Hoffmann, R.; Swenson, J. R.; Gleiter, R. *Chem. Phys. Lett.* **1971**, *10*, 572.

(29) If one again uses 25 kcal/mol as the Cr–N bond energy, then 77% bond dissociation requires 19 kcal/mol. This is not in agreement with the experimental barrier. It may well be the case that our extended Hückel calculations are greatly overestimating the percent dissociation (a 56% loss of the bond energy would be required). The close agreement between our theoretical and experimental results for cis-azo- and pyridazine–Cr(CO)$_5$ argues against this. Equally plausible is that the 25 kcal/mol bond energy is overestimated. There are larger steric factors at work for naphthyridine–Cr(CO)$_5$. In particular the lone pair associated with the uncoordinated nitrogen (at the ground state) overlaps with filled yz and xy. This in turn is reflected in a longer Cr–N distance (2.25 Å compared to 2.10 Å in pyridazine–Cr(CO)$_5$) as well as a lower Cr–N bond dissociation energy (26 kcal/mol for naphthyridine–Cr-(CO)$_5$ vs. 34 kcal/mol for pyridazine–Cr(CO)$_5$). We do *not* trust the magnitude of this Cr–N bond dissociation reduction, but merely note that it is in the expected direction. If the bond dissociation energy was reduced to 20 kcal/mol at the ground state, then a 77% loss of the bond energy would lead to a barrier of 15.4 kcal/mol.

(30) Alvarez, S.; Bermejo, M.-J.; Vinaixa, J. *J. Am. Chem. Soc.*, in press.

(31) (a) Kirtley, S. W. In *Comprehensive Organometallic Chemistry*; Wilkinson, G.; Stone, F. G. A.; Abel, E. W., Eds.; Pergammon: Oxford, England, 1982; Vol. 3, pp 783, 1079, 1255. (b) See also: Marx, D. E.; Lees, A. J. *Organometallics* **1986**, *5*, 2072 and references therein.

phenanthroline. For $n = 1$ and particularly $n = 0$ the lone pairs are swiveled away from each other, which decreases their through-space overlap. However, through-bond conjugation will remain essentially constant,[33] and this should favor a lower barrier. Another attractive ligand system is **23**. Through-bond interaction should remain quite strong, putting n_s above n_a, while through-space overlap is quite weak. Derivatives of **23** including ML_5 complexes are actively being experimentally investigated.[32]

The conclusions we have reached for diazene–$Cr(CO)_5$ complexes should apply equally well to other 18-electron diazene–ML_n types. One major perturbation is introduced in a 16-electron square-planar or trigonal system. Figure 4 presents a Walsh diagram for a generalized diazene ligand where interaction between the lone pairs is absent. The n_s and n_a combinations interact with a hybridized $x^2 - y^2$ (the coordinate system used is shown at the top of Figure 4) metal orbital[12a,c] to produce a M–N σ bond and localized nitrogen lone pair at the ground state. This is identical with the diazene–$Cr(CO)_5$ case (see Figures 1 and 2). At higher energy are the four nonbonding, metal-centered orbitals, which are split in the normal fashion for a square-planar complex.[12a] Finally at a much higher energy there is an empty metal z orbital. An analogous molecular orbital, of course, is present in the diazene–$Cr(CO)_5$ system. However, it is destabilized greatly by one "t_{1u}" component of CO σ. Here it is nonbonding and will figure heavily into the analysis of the rearrangement. On going to the transition state (right side of Figure 4) the xz and xy orbitals remain unchanged. The M–N σ level goes up slightly in energy for the same reasons mentioned previously for diazene–$Cr(CO)_5$. The n_s orbital also overlaps somewhat more with z^2 at the transition state, and this slightly destabilizes it. The major perturbation in this Walsh diagram is that metal z because of its low energy mixes heavily into n_a along with yz. Three molecular orbitals are produced. At low energy $yz + n_a$ is a metal–n_a bonding level where z and yz mix into n_a in a bonding fashion. At very high energy z and yz are antibonding to n_a, $yz - n_a$. In the middle combination, which evolves from yz at the square-planar geometry, n_a is antibonding to yz; however, metal z mixes into this orbital in a manner that is bonding to n_a. The resultant orbital is hybridized away from the diazene ligand. The reader will have noticed that all we have done along this reaction path is to create the splitting pattern for a trigonal bipyramid. For the metal-centered levels, two (xz and xy) are analogous to e'' and the other two (z^2 and yz) are equivalent to e' in a D_{3h} ML_5 complex.[12a] The key feature in this Walsh diagram compared to that in Figure 2 is that, with z^2 as the HOMO, yz does *not* rise to a prohibitively high energy. The repulsion between yz and n_a is alleviated by the empty metal z level. While yz does increase in energy; this is compensated by the stabilization of N_n. The extent of this compensation will, of course, be very sensitive to the relative energy of metal z. The lower it lies in energy, the more it will mix into yz.

The effects of geometrical distortion and lone-pair interaction can easily be incorporated into this model. With the n_a/yz repulsion largely removed, the relative energy of the transition state will now be sensitive to the magnitude of the $n_s/x^2 - y^2$ interaction. Overlap between the two is maximized when the lone pairs point *toward* each other. To evaluate this idea we carried out computations on two hypothetical rearrangements in $(NH_3)_2PtCl_3^-$. In **24** the two nitrogen lone pairs are oriented in parallel directions, whereas in **25** they point toward each other, making a 60° angle. The N⋯N distance in **24** was 2.44 Å while that in **25** was 2.82 Å. These distances were set so that through-space interaction was small and identical in both situations; n_a was 0.2 eV above n_s. The optimal Pt–N distance (to the coordinated NH_3 ligand) was 1.85 Å for both systems at the ground state. At the transition state the optimized Pt–N distances were 2.40 Å for **24** with 63% of the bond energy required to attain it, whereas in **25** the Pt–N distances

24

25
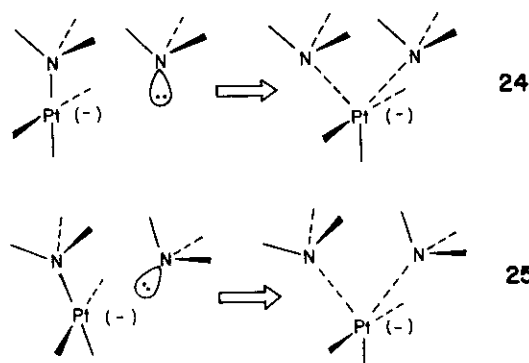
were 2.20 Å and 44% of the bond energy was lost. This is totally consistent with our analysis. The effects of through-bond conjugation will work in the same way as in the $Cr(CO)_5$ complexes; if n_s is destabilized, then the transition state will be more associative. We also note in passing that the rearrangements in 16-electron diazene–ML_3 and –ML_2 should electronically closely resemble metallotropic tautomerizations observed for diazene–main group complexes.[34] The reader is directed to the theoretical work of Alvarez, Bermejo, and Vinaixa, who examined typical reactions.[30]

We have carried out extended Hückel calculations on phenanthroline–, **26**, naphthyridine–, **27**, and pyridazine–$PtCl_3^-$, **28**.

26   **27**   **28**
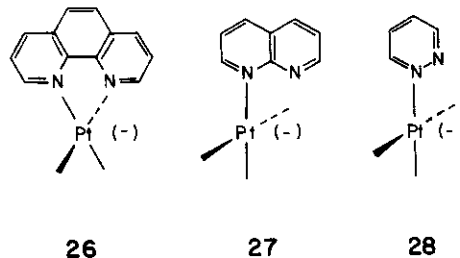
The optimized Pt–N distances were 1.85 Å for **26** and **27** and 1.72 Å for **28**. These are certainly too short. Distances of 2.14 and 2.08 Å have been reported for analogues of **26** and **27**, respectively.[10c,35] Likewise our computed diazene–Pt bond energies appear to be much too large ($\approx$50 kcal/mol for each) although a reliable value appears to be lacking in the literature. At the transition state we predict Pt–N distances of 2.20, 2.40, and 2.16 Å for **26–28**, respectively. The percentage of Pt–N bond energy lost on going from the ground to the transition state was calculated to be 40%, 64%, and 70% for this series. This is in moderately good agreement with experimental data[10b] on phenanthroline–, naphthyridine–, and pyridazine–$Pt(PEt_3)_2Cl^+$ and extended Hückel calculations on the latter two compounds.[30] Experimentally[10b] $\Delta G^\ddagger$ values of <9.5, 12.2, and 17.0 kcal/mol, respectively, have been reported. Our calculations are probably underestimating the dissociative character for the pyridazine complex. Coupling between the diazene ring protons and ^{195}Pt was lost in the fast-exchange limit for pyridazine and phthalazine–$Pt(PEt_3)_2Cl^+$ (where $\Delta G^\ddagger = 18.2$ kcal/mol was found). This implies that the rearrangement mechanism for these two complexes involves complete Pt–N bond rupture. On the other hand, coupling with ^{195}Pt and ^{31}P was retained at the fast-exchange limit for phenanthroline– and naphthyridine–$Pt(PEt_3)_2Cl^+$, which is consistent with an associative mechanism.[10b]

Nucleophilic Substitution and Ligand-Exchange Reactions

It was surprising to us that the transition state for shifting in pyridazine– and naphthyridine–$Cr(CO)_5$ was so dissociative in nature. In fact, the reader will have noticed that the Cr–N distances at the transition state are extremely long and the magnitude of the binding energy between the diazene and $Cr(CO)_5$

(32) Thummel, R. P.; Lefoulon, F.; Mahadevan, R. *J. Org. Chem.* **1985**, *50*, 3824 and references therein. Thummel, R. P., private communications.

(33) For a particularly careful evaluation of through-space and through-bond conjugation as a function of various geometric modifications, see: Hoffmann, R.; Imamura, A.; Hehre, W. J. *J. Am. Chem. Soc.* **1968**, *90*, 1499.

(34) For a comprehensive review see: Fedorov, L. A.; Kravtsov, D. N.; Peregudov, A. S. *Usp. Khim.* **1981**, *50*, 1304; *Russ. Chem. Rev. (Engl. Transl.)* **1981**, *50*, 682.

(35) Bushnell, G. W.; Dixon, K. R.; Khan, M. A. *Can. J. Chem.* **1978**, *56*, 450.

units is computed to be very small. The extended Hückel method has consistently overestimated the binding energy at the ground state, and we can see no reason why this should not be the case for the transition state as well. Therefore, one can reasonably argue that these rearrangements proceed via a 16-electron Cr-(CO)$_5$/noninteracting diazene intermediate caught in the solvent cage. This mechanism is also in agreement with the available experimental data[6a] provided that the rate of Cr(CO)$_5$–diazene collapse is rapid compared to the rate of diazene (or Cr(CO)$_5$) diffusion from the solvent cage, which is likely to be the case here. Mechanistic scenarios quite like this have been amply demonstrated for S$_N$1 reactions in organic chemistry.[36]

As mentioned in the Introduction, the rearrangement in diazene–Cr(CO)$_5$ complexes has a direct bearing on the ligand substitution reaction for 18-electron organometallic complexes. The naphthyridine ligand represents a nearly optimal situation for S$_N$2-like behavior in a ligand-substitution process (in terms of lone-pair orientation and interaction); however, our calculations imply that even here very little bonding remains between Cr(CO)$_5$ and naphthyridine in the transition state. Recent gas-phase work for the attack of bare and partially solvated nucleophiles on Fe-(CO)$_5$ have also shown no evidence for direct, S$_N$2 ligand substitution.[37] Nucleophilic attack, if it occurs at all, is at a carbonyl carbon to initially give an acyl intermediate. On the other hand, despite an occasional uncertainty,[38] the S$_N$2 reaction is pervasive in organic chemistry. The most compelling recent evidence comes from the gas-phase experimental work by Brauman[39] and theoretical simulations of the condensed phase reaction by Joregensen and Chandrasekhar.[40] What is the reason for this difference in reactivity in the organic and organometallic worlds?

In the following discussion it is important to realize that for the ML$_n$ complexes we are addressing, L is a strong σ donor ligand and is *not* a polyene that can slip to a lower coordination number (e.g. cyclopentadienyl, allyl, etc.). Furthermore, the molecules (at the ground state) are saturated, 18-electron ML$_n$ complexes and 8-electron CH$_3$X species.

There are two ways to view this reactivity difference. The transition state for an S$_N$2, X$^-$ + CH$_3$X reaction is the trigonal bipyramid. A particularly simple way to develop the molecular orbitals of the "supermolecule" at the transition state is shown in **29**. Linear combinations of the valence hybrid orbitals on the


29
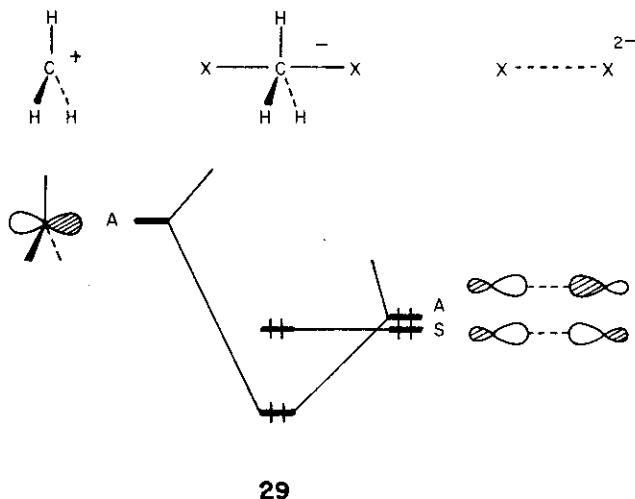
entering nucleophile and leaving group that point toward the central carbon are displayed on the right side of the interaction diagram. For simplicity the leaving group and nucleophile here are regarded as being identical; however, even when this condition is not met, linear combinations of the two will still give two orbitals that have an analogous topology. The 6-electron CH$_3^+$ group has an empty p orbital, which interacts with the A combination to give a filled bonding and empty antibonding molecular orbital. The latter MO along with three C–H bonding orbitals is shown in **30**. These four molecular orbitals describe the bonding between
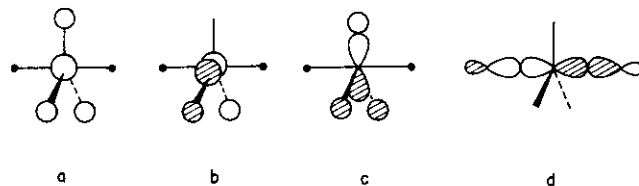
30

the surrounding "ligands" and the central carbon. The S combination in **29** is *nonbonding* between the X---X^{2-} fragment and the central carbon. This model can be carried one step further by noting that the S combination can (and will) overlap with **30a** along with its antibonding counterpart, **31**, to give three new
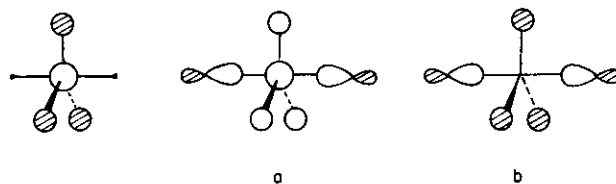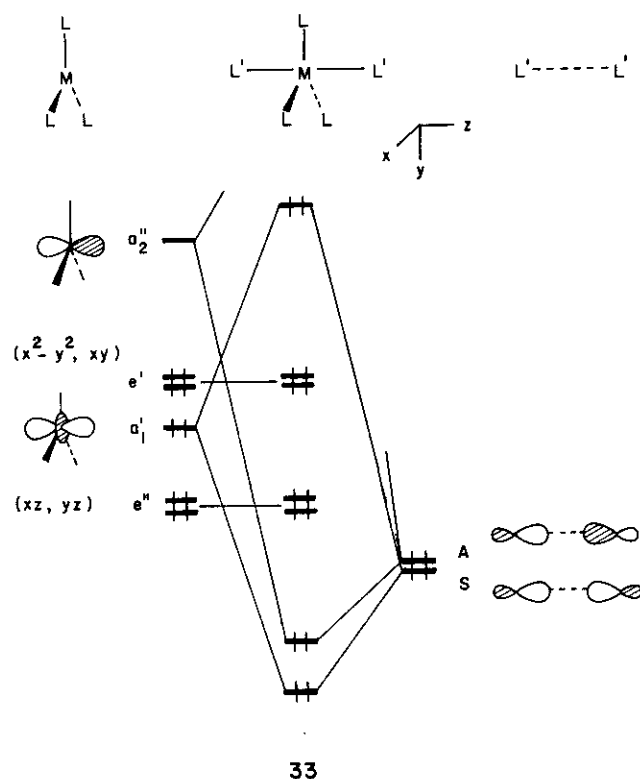

31   **32**

molecular orbitals. The two that are filled are shown in **32**. The relative amounts of **30a** and **31** that mix with the S combination are, of course, variable. That will depend upon the relative energies and exact composition of the three orbitals; thus, **32b** may have a small amount of carbon s character mixed in a bonding or antibonding way to the S lone-pair combination, which in turn will have a geometric and energetic impact on the transition state,[12a,40,42] but this is beyond the scope of our discussion. The important point is that **32b** is nonbonding. Thus, *irrespective of the C–X distances at the transition state*, eight electrons are shared between the surrounding atoms and the central carbon (**30b–d** and **32a**); therefore, the transition state for an S$_N$2 reaction obeys the effective atomic number rule (Lewis octet rule).[41] An equivalent way to put this is that all bonding orbitals between the surrounding ligands and central carbon are filled and the antibonding ones are empty. The essence of this delocalized model, displayed by **30b–d** and **32**, has been of course given before, most notably in the work by Musher, Rundle, and Pimentel on the so-called hypervalent main group compounds.[42] A careful consideration of the electronic factors associated with **30d** and **32b** can be used to rationalize the relative stability of the transition state; however, this is beyond the scope of the work here. The important point is that the transition state can be stabilized to the extent that it becomes the ground state.[43] In an organometallic L' + ML$_{n-1}$L' identity reaction, a nonbonding molecular orbital is *not* formed at the transition state. Consider the situation for $n = 4$ where an 18-electron ML$_3$L' complex reacts with L' via an analogous backside S$_N$2 transit. The molecular orbitals of the trigonal-bipyramidal transition state are developed in **33**. On the left are the valence orbitals of a 16-electron ML$_3$ fragment.[12a,b]

(36) Lowry, T. H.; Richardson, K. S. *Mechanism and Theory in Organic Chemistry*, 2nd ed.; Harper and Row: New York, 1981; pp 302–323 1981.

(37) Lane, K. R.; Sallans, L.; Squires, R. R. *J. Am. Chem. Soc.* **1986**, *108*, 4368. Lane, K. R.; Squires, R. R. *Ibid.* **1986**, *108*, 7187.

(38) See, for example: McLennan, D. J. *Acc. Chem. Res.* **1976**, *9*, 281.

(39) Dodd, J. A.; Brauman, J. I. *J. Am. Chem. Soc.* **1984**, *106*, 5356 and references therein.

(40) Chandrasekhar, J.; Smith, S. F.; Jorgensen, W. L. *J. Am. Chem. Soc.* **1985**, *107*, 154. Chandrasekhar, J.; Jorgensen, W. L. *Ibid.* **1985**, *107*, 2974.

(41) Sidgwick, N. V. *The Electronic Theory of Valency*; Cornell University Press: New York, 1927.

(42) (a) Musher, J. I. *Angew. Chem., Int. Ed. Engl.* **1969**, *8*, 54. (b) Rundle, R. E. *J. Am. Chem. Soc.* **1963**, *85*, 112. (c) Pimentel, G. C. *J. Chem. Phys.* **1951**, *19*, 446.

(43) Forbus, T. R.; Martin, J. C. *J. Am. Chem. Soc.* **1979**, *101*, 5057. Martin, J. C. *Science (Washington, D.C.)* **1983**, *221*, 509.

33

Table I. Parameters Used in the Extended Hückel Calculations

orbital		H_{ii}, eV	ζ_1	ζ_2	$C_1{}^a$	$C_2{}^a$
Cr	3d	−11.22	4.95	1.60	0.4876	0.7205
	4s	−8.66	1.70			
	4p	−5.24	1.70			
Pt	5d	−12.59	6.01	2.70	0.6334	0.5513
	6s	−9.08	2.55			
	6p	−5.48	2.55			
Cl	3s	−26.30	2.033			
	3p	−14.20	2.033			
C	2s	−21.40	1.625			
	2p	−11.40	1.625			
N	2s	−26.0	1.950			
	2p	−13.4	1.950			
O	2s	−32.30	2.275			
	2p	−14.80	2.275			
H	1s	−13.60	1.30			

^{a} Contraction coefficients used in the double-ζ expansion.

The A combination of L′---L′ interacts with metal z to form filled bonding and empty antibonding molecular orbitals. The S combination interacts with metal z^2 to form bonding and antibonding levels, *of which both are filled*. To be sure, an orbital analogous to **30a** mixes in an antibonding fashion to the S combination while an orbital analogous to **31** mixes in a bonding way into both of these molecular orbitals; however, the net result of these secondary mixings is cancellation just as in the organic example. Thus, we are left with the picture shown in **33**; there will always be a strong repulsion between filled z^2 and the S combination that does not exist in the organic world. This repulsion intrinsically disfavors an associative, S_N2 transition state for organometallic compounds. A front-side displacement passing through a square-pyramidal transition state as well as a structure with lower symmetry on the five-coordinate manifold[12a,44] shows an identical feature. One metal-surrounding ligand antibonding molecular orbital is always formed in this 20-electron species. The same situation occurs for front-side displacement in ML_5L'; see the right side of Figure 1 where yz–n_a can easily be identified as the metal–ligand antibonding orbital. This is also found for any other seven-coordinate geometry.[45]

The reactivity difference for nucleophilic substitution in organometallic and organic molecules can also be viewed from a slightly different perspective. Consider the early stages for the attack of X⁻ on CH_3X. There will be some initial repulsion between the lone pair(s) on X⁻ and filled C–H bonding orbitals, which is alleviated to some extent as the molecule undergoes the Walden inversion process. This is also the case for attack of a nucleophile on any ML_n complex. The essential difference is derived from the fact that for any saturated, 18-electron complex there is a set of filled metal d orbitals that are directed in regions of the molecule between the surrounding ligands (the t_{2g} set in ML_6, see the left side of Figure 1, the e' and e'' levels in ML_5, see **33**, or the t_2 + e set in ML_4[12a,b]). Therefore, lone-pair–lone-pair repulsion between the nucleophile and metal is also turned on. This repulsive interaction ultimately translates into the occupation

of a metal–ligand antibonding orbital at the transition state for an S_N2 pathway.

Using either line of reasoning, we can easily establish from Figure 4 and the discussion around it that an S_N2 mechanism (with a reasonable amount of associative character or even a discrete five-coordinate intermediate in terms of an A mechanism) is possible for a 16-electron square-planar complex. Our results for pyridazine–, naphthyridine–, and phenanthroline–$PtCl_3^-$ bear this out. The situation for nucleophilic attack at ML_n complexes when L is a weak σ-donor ligand (e.g. H_2O, NH_3, etc.) is radically different from that presented here. This topic shall be addressed elsewhere.[46] Likewise, the preferred mechanism when one ligand is a nitrosyl or polyene[2] is a subject for future investigations.

Appendix

The Cr–C, C–O, N–H, and Pt–Cl distances were fixed at 1.84, 1.14, 0.99, and 2.35 Å, respectively. All calculations employed Cr–C–O angles of 180°, and the diazene rings were idealized with C–C and C–N distances of 1.41 Å. The N–N distances of H_2N_2 were fixed at 1.25 and 1.366 Å for η^1 and η^2 geometries, respectively, at the extended Hückel level. They were optimized at the ab initio level. The extended Hückel calculations[47] used a modified Wolfsberg–Helmholz formula[48] with the parameters listed in Table I as taken from previous work.[12c,49] The ab initio calculations utilized the GAMESS package.[50] The Cr basis started from Huzinaga's (4333/43/4) primitive set.[51] The d along with 4s and augmented 4p functions were replaced by ones optimized for molecular environments[52,53] to yield a basis set of the form (4333/433/31). The standard 3-21G basis[54] was used for H, C, N, and O atoms.

(44) (a) Rossi, A. R.; Hoffmann, R. *Inorg. Chem.* **1975**, *14*, 365. (b) Hoffmann, R.; Chen, M. M. L.; Elian, M.; Rossi, A. R.; Mingos, D. M. P. *Ibid.* **1974**, *13*, 2666.

(45) Hoffmann, R.; Beier, B. F.; Muetterties, E. L.; Rossi, A. R. *Inorg. Chem.* **1977**, *16*, 511.

(46) Kang, S. K.; Lam, B.; Albright, T. A.; O'Brien, J. F., manuscript in preparation.

(47) Hoffmann, R. *J. Chem. Phys.* **1963**, *39*, 1397. Hoffmann, R.; Lipscomb, W. N. *Ibid.* **1962**, *36*, 2179; **1962**, *37*, 2872.

(48) Ammeter, J. H.; Bürgi, H. B.; Thibeault, J. C.; Hoffmann, R. *J. Am. Chem. Soc.* **1978**, *100*, 3686.

(49) Albright, T. A.; Hofmann, P.; Hoffmann, R. *J. Am. Chem. Soc.* **1977**, *99*, 7546.

(50) Dupuis, M.; Spangler, D.; Wendoloski, J. J. *National Resource for Computations in Chemistry Software Catalog*; 1980; Vol. 1, Program QG01.

(51) Huzinaga, S.; Andzelm, J.; Klobukowski, M.; Radzio-Andzelm, E.; Sakai, Y.; Tatawaki, H. *Gaussian Basis Sets for Molecular Calculations*; Elsevier: Amsterdam, 1984.

(52) Rappe, A. K.; Smedley, T. A.; Goddard, W. A., III. *J. Phys. Chem.* **1981**, *85*, 2607.

(53) Pietro, W. J.; Hehre, W. J. *J. Comput. Chem.* **1983**, *4*, 241.

(54) Binkley, J. S.; Pople, J. A.; Hehre, W. J. *J. Am. Chem. Soc.* **1980**, *102*, 939.